frontiers | Frontiers in Energy Research

TYPE Original Research
PUBLISHED 11 July 2024
DOI 10.3389/fenrg.2024.1411152

OPEN ACCESS

EDITED BY
Zening Li,
Taiyuan University of Technology, China

REVIEWED BY
Zhenning Pan,
South China University of Technology, China
Zhiwei Li,
North China Electric Power University, China

*CORRESPONDENCE
Zhihui Zhang,
zhangzhihui@epri.sgcc.com.cn

RECEIVED 02 April 2024
ACCEPTED 15 May 2024
PUBLISHED 11 July 2024

CITATION
Zhang Z, Yang S, Ma Y, Sun S, Yu P and Yang F (2024), Constrained distributionally robust optimization for day-ahead dispatch of rural integrated energy systems with source and load uncertainties.
Front. Energy Res. 12:1411152.
doi: 10.3389/fenrg.2024.1411152

Constrained distributionally robust optimization for day-ahead dispatch of rural integrated energy systems with source and load uncertainties

Zhihui Zhang[1]*, Song Yang[2], Yunting Ma[1], Shumin Sun[2], Peng Yu[2] and Fei Yang[1]

[1]State Grid Shanghai Energy Internet Research Institute Co. Ltd., Shanghai, China, [2]State Grid Shandong Electric Power Company Electric Power Science Research Institute, Jinan, China

As a deep connection between agriculture and energy, the rural integrated energy system (RIES) is a micro-scale supply–distribution–storage–demand network, which provides an important means to realize the utilization of rural clean energy. This paper proposes a day-ahead scheduling model of the RIES to improve its economical effectiveness, where three energy carriers, namely, biogas, electric power, and heat, are integrated. To address the source and load uncertainties composed of photovoltaic power, power load, and heat load, this paper develops a constrained distributionally robust optimization (CDRO), which optimizes the cost expectation related to the extreme distribution to enhance the robustness, while limiting the loss of cost expectation in the historical distribution to ensure economical effectiveness. In addition, an ambiguous set of the source and load uncertainties incorporating 1-norm and infinity-norm constraints is established, which realizes a flexible adjustment for the conservativeness of CDRO. The distributionally robust dispatch is formulated as a deterministic programming in a two-stage solving framework, where the subproblem uploads its extreme probability distribution to the master problem, and these two problems are iteratively optimized until the convergence. Finally, the numerical simulations in a modern farm park prove the performance of the constructed dispatch model and the flexibility of CDRO in balancing the economical effectiveness and robustness of the dispatch.

KEYWORDS

rural integrated energy system, day-ahead dispatch, source and load uncertainties, distributionally robust optimization, two-stage optimization

1 Introduction

To meet the national strategical demand of rural revitalization, clean, low-carbon, and rich-reserve biomass energy is being rapidly developed and utilized in China. It is estimated that in China, by 2030, the installed capacity of biomass plants will reach 52 GW, which can provide more than 330 billion KWh of clean electric power every year (Liang et al., 2024). In addition, the distributed rooftop photovoltaic power generation has also developed into a new trend of rural green development. As a deep connection between agriculture and energy, the rural integrated energy system (RIES) is a micro-scale

supply–distribution–storage–demand system, which provides an important means to realize the utilization of rural clean energy. Day-ahead optimal dispatch (Seyednouri et al., 2023) which plays a crucial part in decreasing the operating cost of the RIES and enhancing use of biomass and renewable energies needs more attention.

Recently, many scholars have studied the optimal operation of the RIES. Ma and Fu (2021) studied the coupling principle of agriculture, meteorology, and energy and introduced the advanced applications corresponding to the coupling. Fu et al. (2020) explores the security problems caused by the connection of energy and agriculture and summarizes the security technology to ensure the double security of energy and food. The above research studies conclude the current construction status and development trend of the RIES; however, these research studies have not discussed the technical details for the optimal operation of the RIES. Zhou et al. (2018) established a multi-energy coupling model to clarify the effect of fermentation under external energy injection. Wu et al. (2021) established a novel model for a biogas–solar–wind-based integrated energy system and developed an improved realization of the multitasking paradigm using multiobjective optimization. Yu and Yin (2023) promoted carbon capture technologies for waste power generation in the RIES. Yu et al. (2022) developed a three-participator game mechanism for the RIES considering the interests of the government, farmers, and new energy enterprises to realize optimal and clean operation of the system. However, the aforementioned studies are deterministic optimization that ignores the randomness of photovoltaic power, power, and heat load. The above source and load uncertainties directly influence the intraday power balance, and the dispatch plan obtained from the deterministic dispatch model cannot guarantee the economy of the RIES in intraday operation.

With the deployment of renewable energies, the optimization of integrated energy systems combined with multiple uncertainties has gradually attracted the attention of scholars. Currently, the strategies to cope with uncertainties mainly include stochastic optimization (SO)-based methods and robust optimization (RO)-based methods. SO randomly extracts scenarios with respect to the empirical probability distribution of uncertainty conditions and then establishes the security constraints for each sample scenario and optimizes the operating cost expectation of these sample scenarios (Xu et al., 2017). Jani et al. (2022) adopted the probability distribution function to describe the uncertainty, and the scenario-oriented SO is applied. The scenario-oriented stochastic method is also adopted by Eghbali et al. (2022) to deal with the uncertainty of electric vehicles. However, discrete sample scenarios cannot cover the continuous uncertainty distributions, and it is hard for SO to guarantee secure operation in all scenarios. In addition, the true distribution of the source and load uncertainties does not precisely obey the empirical probability distribution, and, as a result, the robustness of SO under other distributions is affected.

RO models uncertainty conditions using continuously distributed maximum domains and deals with extreme uncertainty conditions using dual theory to ensure the robustness of the dispatch plan. Traditional RO establishes the uncertainty set to formulate the maximum domain of uncertain scenarios and optimizes the operating cost of microgrids under extreme scenarios (Liu et al., 2018; Bolurian et al., 2022; Tan et al., 2022). The widely adopted modeling methods for the uncertainty set include box-based and polyhedron-based sets (Bertsimas et al., 2013). In addition, Zhao et al. (2021) developed an ellipsoid-based uncertainty set to reduce the conservativeness of TRO. Nevertheless, since the probability of extreme scenarios is extremely low, RO is generally very conservative. Compared to RO, the recent widely used distributionally robust optimization (DRO) is less conservative (Zuo et al., 2023). DRO uses the ambiguous set to describe the maximum domain of uncertain probability distributions and minimizes the operating cost expectation under extreme distributions. Siqin (2022) established an ambiguous set for wind and photovoltaic power based on Wasserstein distance and developed a DRO operation of the microgrid considering both power-to-gas and CHP units. Zhang (2022) utilized the multiorder moment information to formulate the ambiguous set of uncertain variables and established a distributionally robust economic operation model for a multi-energy coupled microgrid. Zhai et al. (2022) proposed a DRO-based chance-constrained model for the multi-energy microgrid, and an optimal additional approximation is developed to convert the model to a tractable form. However, the above studies approximate the second-stage decision of microgrids as the affine policy (Qu et al., 2022) to make the DRO tractable; the affine policy restricts the optimization space of recourse actions and significantly affects the economical effectiveness of the dispatch decision. To achieve the optimum, Wei et al. (2016) proposed a dual vertex generation-based two-stage method for adaptive optimization-based distributionally robust optimization, and Zheng et al. (2021) developed an extreme distribution generation-based solution for the complex DRO. However, the solution process of the dual vertex generation-based method or the extreme distribution generation-based method is too complicated, and nonlinear constraints will be generated by the product of uncertain parameters and dual variables.

Recently, a new data-driven DRO method is being developed rapidly, which extracts a certain number of reference samples from the large-scale available historical data and establishes the 1-norm and infinity-norm-based probability density sets to describe the distribution of the uncertainties (Ding et al., 2017). The method has the below advantages: 1) it directly makes full use of the historical observation, rather than the moment information representing the overall performance. 2) The dualization is not required, and thus, the solution procedure is relatively effortless. However, the existing probability density set-based method only focuses on the expected objective under the extreme distribution. The historical distribution generated from the historical observation probably approaches the real distribution of uncertainties, and hence, the cost expectation under the historical distribution deserves more attention. This paper combines the principle of SO and DRO, and the contributions are listed as follows:

1) A novel day-ahead dispatch model of the RIES is established. Three energy carriers, namely, biogas, electric power, and heat, are integrated in the RIES. In addition, the economic operation of the RIES is realized through cooperative regulation of photovoltaic power, biogas generator, heat pump, electric boiler, transferable power load, power, and heat storage, where the diversified regulation resources are modeled accurately.

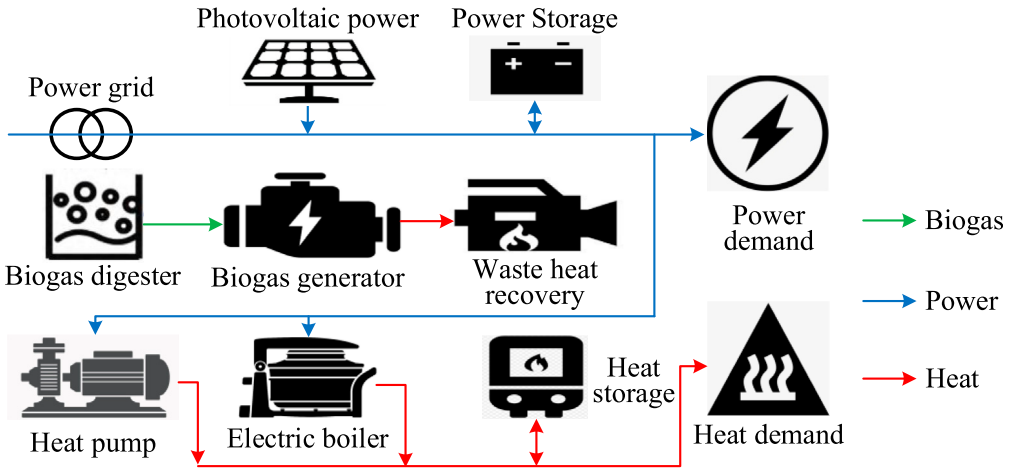

FIGURE 1
Framework of the rural integrated energy system.

2) A novel constrained distributionally robust optimization (CDRO) is developed to address source and load uncertainties in the RIES. The principle is to minimize the operating cost expectation in the extreme distribution to enhance the robustness, while further limiting loss of cost expectation in the historical distribution to ensure economical effectiveness. The balance between the robustness and economical effectiveness can be realized through reasonably setting an equilibrium coefficient.
3) A tailored two-stage solution procedure is developed for the proposed distributionally robust dispatch. First, the absolute value constraint in the ambiguous set is convexified. Then, a column and constraint generation (C&CG) method is introduced to solve the convexified problem. The master problem determines the day-ahead decision variables against all known extreme distributions of the probability density. The subproblem receives the obtained decision variables and determines an extreme distribution of the probability density and adds it to the master problem.

The rest of this paper is organized as follows: Section 2 models the distributionally robust day-ahead dispatch of the RIES. Section 3 presents the tailored two-stage solution procedure to solve the dispatch problem. Section 4 describes the numerical simulations and analysis on a modern farm park. Section 5 provides the conclusion of this paper.

2 Distributionally robust day-ahead dispatch of the RIES

The frame of the constructed RIES is displayed in Figure 1. The energy carrier in the system contains electric power, heat, and biogas. The biogas is generated by the biogas digester and can be stored in the biogas storage. The biogas is fed into the biogas generator to produce electric power and heat. The electric power is produced from the power grid, photovoltaic power, and biogas generator and fed into the heat pump and electric boiler to generate heat, and it can be stored in power storage. The heat is produced by waste heat recovery of the biogas generator and electric boiler and can be stored in heat storage. Finally, the demand of the system includes power load and heat load.

2.1 Day-ahead and intraday operation problem

The distributionally robust day-ahead dispatch is a typical two-stage problem. The day-ahead problem in the first stage is a pre-decision problem, which determines the trading power from the power grid. The intraday operation in the second stage is a regulation problem, which adjusts the intraday trading power and the scheduling plan of the regulating resources to minimize the intraday operating cost.

First stage (day-ahead): in this stage, the RIES trades power from the operator, and the power transaction cost is minimized, i.e.,

$$F_1 = \min \sum_t p_t P_t^{\mathrm{tr}}, \tag{1}$$

$$\underline{P}^{\mathrm{tr}} \le P_t^{\mathrm{tr}} \le \bar{P}^{\mathrm{tr}}, \tag{2}$$

where P_t^{tr} is the day-ahead trading power, p_t is the power price, and $\bar{P}^{\mathrm{tr}}/\underline{P}^{\mathrm{tr}}$ are the upper/lower restrictions of P_t^{tr}, respectively.

The first-stage problem can be refined as follows:

$$\min_{\boldsymbol{x}\in\mathcal{X}} \boldsymbol{c}^{\top}\boldsymbol{x}, \tag{3}$$

where $\boldsymbol{x}\in\chi$ are decision variables in the first stage, i.e., the day-ahead trading power P_t^{tr}, and $\boldsymbol{c}$ are day-ahead cost coefficients.

Second stage (intraday operation): in this stage, the RIES adjusts the intraday trading power and the dispatch plan of power storage, transferable power load, biogas generator, biogas storage, heat pump, electric boiler, and heat storage. The intraday operating cost includes the intraday power trading cost, material cost of the biogas generator, and the cost of the transferable power load:

$$\begin{aligned} F_2 = \min \quad & \sum_t \left(b_t^{+}\Delta P_t^{\mathrm{tr},+} + b_t^{-}\Delta P_t^{\mathrm{tr},-}\right) + \sum_t b_t^{\mathrm{g}} G_t \\ & + \sum_t \left(d_t^{+}\Delta P_t^{\mathrm{dr},+} + d_t^{-}\Delta P_t^{\mathrm{dr},-}\right), \end{aligned} \tag{4}$$

where $\Delta P_t^{\mathrm{tr},+}/\Delta P_t^{\mathrm{tr},-}$ are the intraday purchase and sell power from/to the power grid, respectively; G_t is the biogas input of the biogas generator; $\Delta P_t^{\mathrm{dr},+}/\Delta P_t^{\mathrm{dr},-}$ are the upward and downward regulated power of transferable power load, respectively; b_t^+/b_t^- are the transaction price for the intraday purchase and sell power, respectively; b_t^{g} is the material cost coefficient of the biogas generator, and d_t^+/d_t^- are the upward and downward cost coefficients of the transferable power load, respectively.

The following security constraints need to be met for the second-stage intraday operation of the RIES.

2.1.1 Photovoltaics and demands

$$\begin{cases} P_t^{\mathrm{v}} = \tilde{P}_t^{\mathrm{v}} + u_t^{\mathrm{v}} \\ P_t^{\mathrm{d}} = \tilde{P}_t^{\mathrm{d}} + u_t^{\mathrm{p}} \\ H_t^{\mathrm{d}} = \tilde{H}_t^{\mathrm{d}} + u_t^{\mathrm{h}} \end{cases}, \tag{5}$$

where the real photovoltaic power output P_t^{v}, power load P_t^{d}, and heat load H_t^{d} equal the sum of the forecast value and power/heat fluctuation.

2.1.2 Biogas generator

$$P_t^{\mathrm{g}} = \eta^{\mathrm{p}} H G_t, H_t^{\mathrm{g}} = \eta^{\mathrm{h}} H G_t, \tag{6}$$

$$\underline{P}^{\mathrm{g}} \le P_t^{\mathrm{g}} \le \bar{P}^{\mathrm{g}}, \tag{7}$$

where H is the calorific value of biogas; P_t^{g} and H_t^{g} are the power and afterheat produced by the biogas generator, respectively; and η^{p} and η^{h} are the power generating efficiency and afterheat efficiency of the biogas generator, respectively. $\bar{P}^{\mathrm{g}}/\underline{P}^{\mathrm{g}}$ are the upper/lower restrictions of P_t^{g}.

2.1.3 Waste heat recovery

The heat export of the device does not exceed the afterheat of the biogas generator.

$$0 \le H_t^{\mathrm{w}} \le H_t^{\mathrm{g}}, \tag{8}$$

where H_t^{w} is the heat export of the waste heat recovery.

2.1.4 Electric boiler

$$H_t^{\mathrm{b}} = \eta^{\mathrm{b}} P_t^{\mathrm{b}}, \tag{9}$$

$$0 \le H_t^{\mathrm{b}} \le \bar{H}^{\mathrm{b}}, \tag{10}$$

where η^{b} is the conversion efficiency and H_t^{b} and P_t^{b} are the heat output and power input of the electric boiler, respectively.

2.1.5 Transferable power load

$$\begin{cases} 0 \le \Delta P_t^{\mathrm{dr},+} \le \Delta \bar{P}_t^{\mathrm{dr},+} \\ 0 \le \Delta P_t^{\mathrm{dr},-} \le \Delta \bar{P}_t^{\mathrm{dr},-} \end{cases}, \forall t \in T_{i,\mathrm{A}}, \tag{11}$$

$$\Delta P_t^{\mathrm{dr},+} = 0, \Delta P_t^{\mathrm{dr},-} = 0, \forall t \in T_{i,\mathrm{B}}, \tag{12}$$

$$P_t^{\mathrm{dr},0} + \Delta P_t^{\mathrm{dr},+} - \Delta P_t^{\mathrm{dr},-} \ge 0, \tag{13}$$

$$\sum\nolimits_t \left(\Delta P_t^{\mathrm{dr},+} - \Delta P_t^{\mathrm{dr},-}\right) = 0, \tag{14}$$

where $\Delta P_t^{\mathrm{dr},+}$ and $\Delta P_t^{\mathrm{dr},-}$ are the upregulated and downregulated power of transferable power load, respectively. $T_{i,\mathrm{A}}$ is the set of transferable periods, $T_{i,\mathrm{B}}$ is the set of non-transferable periods, and Equation 14 shows that the summation of transferred power load equals the original demand.

2.1.6 Power storage

$$0 \le P_t^{\mathrm{s},+} \le \bar{P}^{\mathrm{s},+}, \tag{15}$$

$$0 \le P_t^{\mathrm{s},-} \le \bar{P}^{\mathrm{s},-}, \tag{16}$$

$$S_t^{\mathrm{p}} = S_{t-1}^{\mathrm{p}} + \eta^{\mathrm{p},+} P_t^{\mathrm{s},+} \Delta t - \frac{P_t^{\mathrm{s},-}}{\eta^{\mathrm{p},-} \Delta t}, \tag{17}$$

$$\underline{S}^{\mathrm{p}} \le S_t^{\mathrm{p}} \le \bar{S}^{\mathrm{p}}, \tag{18}$$

$$S_T^{\mathrm{p}} = S_0^{\mathrm{p}}, \tag{19}$$

where $P_t^{\mathrm{s},+}, P_t^{\mathrm{s},-}$ are the charge–discharge power of the power storage, $\bar{P}^{\mathrm{s},+}/\bar{P}^{\mathrm{s},-}$ are the upper restrictions of the charge–discharge power, S_t^{p} is the stored power, $\eta^{\mathrm{p},+}/\eta^{\mathrm{p},-}$ are the charge–discharge efficiency, and $\bar{S}^{\mathrm{p}}/\underline{S}^{\mathrm{p}}$ are the upper/lower restrictions of the stored power, respectively; Equation 19 indicates that the stored power after the dispatch is resumed to the initial state.

2.1.7 Heat storage

$$0 \le H_t^{\mathrm{s},+} \le \bar{H}^{\mathrm{s},+}, \tag{20}$$

$$0 \le H_t^{\mathrm{s},-} \le \bar{H}^{\mathrm{s},-}, \tag{21}$$

$$S_t^{\mathrm{h}} = (1-\rho) S_{t-1}^{\mathrm{h}} + \eta^{\mathrm{h},+} H_t^{\mathrm{s},+} \Delta t - \frac{H_t^{\mathrm{s},-}}{\eta^{\mathrm{h},-} \Delta t}, \tag{22}$$

$$\underline{S}^{\mathrm{h}} \le S_t^{\mathrm{h}} \le \bar{S}^{\mathrm{h}}, \tag{23}$$

$$S_T^{\mathrm{h}} = S_0^{\mathrm{h}}, \tag{24}$$

where $H_t^{\mathrm{s},+}, H_t^{\mathrm{s},-}$ are the charge–discharge heat of the heat storage, $\bar{H}^{\mathrm{s},+}/\bar{H}^{\mathrm{s},-}$ are the upper restrictions of the charge–discharge heat, S_t^{h} is the stored heat, ρ is the heat loss rate, and $\bar{S}^{\mathrm{h}}/\underline{S}^{\mathrm{h}}$ are the upper/lower restrictions of the stored heat, respectively; Equation 24 indicates that the stored heat after the dispatch is resumed to the initial state.

2.1.8 Power and heat balance

$$P_t^{\mathrm{tr}} + \Delta P_t^{\mathrm{tr},+} - \Delta P_t^{\mathrm{tr},-} + P_t^{\mathrm{v}} + P_t^{\mathrm{g}} = P_t^{\mathrm{d}} + P_t^{\mathrm{b}} + P_t^{\mathrm{dr},0} + \Delta P_t^{\mathrm{dr},+} - \Delta P_t^{\mathrm{dr},-} + P_t^{\mathrm{s},+} - P_t^{\mathrm{s},-}, \tag{25}$$

$$H_t^{\mathrm{w}} + H_t^{\mathrm{b}} = H_t^{\mathrm{d}} + H_t^{\mathrm{s},+} - H_t^{\mathrm{s},-}, \tag{26}$$

The second-stage problem is refined as follows:

$$\begin{aligned} &Q(\boldsymbol{x}, \boldsymbol{u}) = \min_{\boldsymbol{y}} \boldsymbol{f}^{\top} \boldsymbol{y} \\ &\text{s.t.} \quad \boldsymbol{G}\boldsymbol{y} \le \boldsymbol{g} \\ &\boldsymbol{A}\boldsymbol{x} + \boldsymbol{B}\boldsymbol{y} + \boldsymbol{C}\boldsymbol{u} = \boldsymbol{d} \end{aligned}, \tag{27}$$

where $\boldsymbol{y}$ is the intraday decision variables; $\boldsymbol{f}$ is intraday cost coefficients; and $\boldsymbol{G}$, $\boldsymbol{A}$, $\boldsymbol{B}$, $\boldsymbol{C}$, $\boldsymbol{g}$, and $\boldsymbol{d}$ are the constant matrices

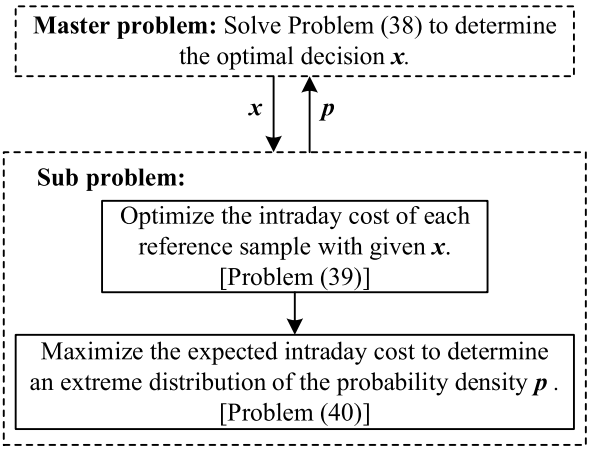

FIGURE 2
Computing framework of the two-stage solution.

and vectors, respectively. The intraday decision $\boldsymbol{y}$ includes the power and afterheat produced by the biogas generator (P_t^{g}; H_t^{g}), heat export of the waste heat recovery H_t^{w}, heat output and power input of the electric boiler (H_t^{b}; P_t^{b}), upregulated and downregulated power of transferable power load ($\Delta P_t^{\mathrm{dr},+}$; $\Delta P_t^{\mathrm{dr},-}$), charge–discharge power and stored power of the power storage ($P_t^{\mathrm{s},+}, P_t^{\mathrm{s},-}, S_t^{\mathrm{p}}$), and charge–discharge heat and stored heat of the heat storage ($H_t^{\mathrm{s},+}, H_t^{\mathrm{s},-}, S_t^{\mathrm{h}}$).

2.2 Robust form of the dispatch model

In the proposed dispatch model of the RIES, the photovoltaic power output fluctuation u_t^{v}, the power load u_t^{P}, and the thermal load fluctuation u_t^{h} are uncertain variables, and they constitute the source and load uncertainties. The day-ahead scheduling model is essentially a two-stage problem, which optimizes the day-ahead operating cost in the first stage and the expectation of the intraday cost in the second stage. In addition, since the possibility for the occurrence of the extreme distribution is relatively low, we further limit the loss of the cost expectation in the historical distribution to reduce the conservativeness of the distributionally robust dispatch. The constrained distributionally robust day-ahead dispatch can be refined as shown below:

$$\begin{aligned} &\min_{\boldsymbol{x}\in\mathcal{X}} \max_{p\in\mathcal{P}} \boldsymbol{c}^{\top}\boldsymbol{x} + \mathbb{E}_p[Q(\boldsymbol{x},\boldsymbol{u})] \\ &\text{s.t. } \boldsymbol{c}^{\top}\boldsymbol{x} + p_{k,0}Q(\boldsymbol{x},\boldsymbol{u}_k) \le \bar{F} \end{aligned}, \tag{28}$$

where P and $\mathcal{P}$ are the probability and the ambiguous set of the source and load uncertainties, respectively; $p_{k,0}$ is the baseline probability density of the kth reference sample $\boldsymbol{u}_k$; and $\bar{F}$ is the allowed maximum for the cost expectation in the historical distribution.

The maximum limit $\bar{F}$ can be predefined as shown below:

$$\begin{cases} \bar{F} = \underline{F}_{\mathrm{emp}} + \lambda\left(\bar{F}_{\mathrm{emp}} - \underline{F}_{\mathrm{emp}}\right) \\ \underline{F}_{\mathrm{emp}}\colon \min_{\boldsymbol{x}\in\mathcal{X}} \boldsymbol{c}^{\top}\boldsymbol{x} + p_{k,0}Q(\boldsymbol{x},\boldsymbol{u}_k) \\ \bar{F}_{\mathrm{emp}}\colon \min_{\boldsymbol{x}\in\mathcal{X}} \max_{p\in\mathcal{P}} \boldsymbol{c}^{\top}\boldsymbol{x} + \mathbb{E}_p[Q(\boldsymbol{x},\boldsymbol{u})] \end{cases}, \tag{29}$$

where $\underline{F}_{\mathrm{emp}}$ is the empirical cost expectation obtained by SO, while $\bar{F}_{\mathrm{emp}}$ is the empirical cost expectation obtained by DRO without the constraint of the empirical cost expectation, and λ is the equilibrium coefficient. The equilibrium coefficient λ locates within [0, 1], which means that the robustness of CDRO is between DRO and SO. The CDRO is close to DRO and pursues the robustness in extreme distributions when λ moves toward 1, while the CDRO is close to SO and pursues the economical effectiveness in the historical distribution (the common distributions) when λ moves toward 0. Therefore, the equilibrium coefficient λ can be set reasonably to achieve a tradeoff between the robustness and economical effectiveness.

We formulate the ambiguous set for the source and load uncertainties according to the confidence set theory. K discrete reference samples can be selected from the M historical observations to characterize the possible value of the source and load uncertainties, and the corresponding baseline probability density is obtained. However, the actual probability distribution values of each reference sample are still uncertain, and we can use the probability density uncertainty to describe the uncertainty of the source–demand distribution. We can construct a set with the baseline density of reference samples as the center and the two sets of 1-norm and infinity-norm as the constraints to restrict the actual probability density of source–demand scenarios. Therefore, the ambiguous set of the source and load uncertainties is formulated as follows:

$$\mathcal{P}\left\{ p_k \left| \begin{array}{l} 0 \le p_k \le 1, \forall k \\ \sum_k p_k = 1 \\ \left|p_k - p_{k,0}\right| \le \theta_{\infty}, \forall k \\ \sum_k \left|p_k - p_{k,0}\right| \le \theta_1 \end{array} \right.\right\}, \tag{30}$$

where p_k is the actual probability of the reference sample k and θ_{∞} and θ_1 are the maximum gap of the probability density under the infinity-norm and 1-norm restrictions, respectively.

The maximum gap of the probability density θ_{∞} and θ_1 can be determined according to the confidence level (Ding et al., 2017).

$$\Pr\left\{\left|p_k - p_{k,0}\right| \le \theta_{\infty}, \forall k\right\} \ge 1 - 2Ke^{-2M\theta_{\infty}}, \tag{31}$$

$$\Pr\left\{\sum_k \left|p_k - p_{k,0}\right| \le \theta_1\right\} \ge 1 - 2Ke^{-\frac{2M\theta_1}{K}}, \tag{32}$$

Let α_{∞} and α_1 denote the confidence level associated with the right hand of the above equations, and then:

$$\theta_{\infty} = \frac{1}{2M}\ln\frac{2K}{1-\alpha_{\infty}}, \theta_1 = \frac{K}{2M}\ln\frac{2K}{1-\alpha_1}. \tag{33}$$

Since the scenarios of the source and load uncertainties are denoted with the reference samples, while the probability density of these reference samples is uncertain, the distributionally robust dispatch Equation 28 is reformulated as follows:

$$\begin{aligned} &\min_{\boldsymbol{x}\in\mathcal{X}} \left\{ \boldsymbol{c}^{\top}\boldsymbol{x} + \max_{p_k\in\mathcal{P}} \sum_k p_k Q(\boldsymbol{x},\boldsymbol{u}) \right\}. \\ &\text{s.t. } \boldsymbol{c}^{\top}\boldsymbol{x} + p_{k,0}Q(\boldsymbol{x},\boldsymbol{u}_k) \le \bar{F} \end{aligned} \tag{34}$$

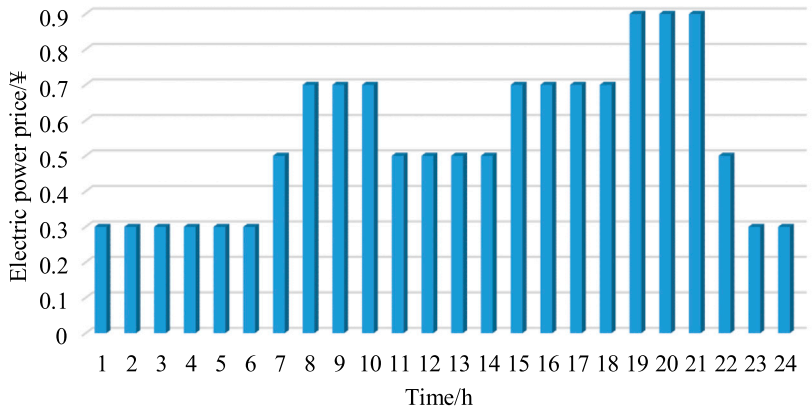

FIGURE 3
Day-ahead power price.

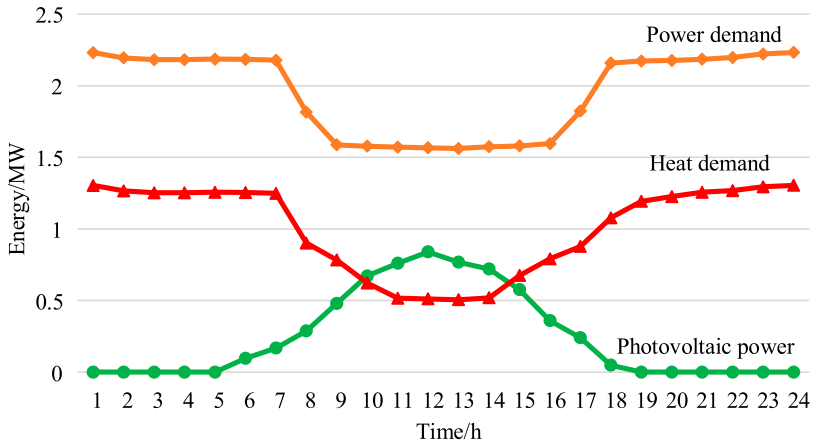

FIGURE 4
Prediction of photovoltaic power, power load, and heat load.

3 Solution method

3.1 Linearization for the absolute value constraint

First, we introduce auxiliary variables to linearize the absolute value constraint in the ambiguous set:

$$\left|p_k - p_{k,0}\right| \le \Delta p_k \quad \downarrow \tag{35}$$

$$-\Delta p_k \le p_k - p_{k,0} \le \Delta p_k, \Delta p_k \ge 0, \tag{36}$$

where Δp_k is the introduced auxiliary variable.

Therefore, the ambiguous set is reformulated into

$$\mathcal{P}\left\{ p_k \left| \begin{array}{l} 0 \le p_k \le 1, \Delta p_k \ge 0, \forall k \\ -\Delta p_k \le p_k - p_{k,0} \le \Delta p_k, \forall k \\ \sum_k p_k = 1 \\ \Delta p_k \le \theta_\infty, \forall k \\ \sum_k \Delta p_k \le \theta_1 \end{array} \right. \right\}. \tag{37}$$

3.2 Two-stage optimization procedure

The constrained distributionally robust dispatch in Equation 28 is a typical two-stage optimization problem, and we develop a C&CG-based decomposition solution for the problem. The principle of the method is to split the two-stage optimization to independently solve the master problem and subproblem. The master problem determines the day-ahead decision variables against all known extreme distributions of the probability density. The subproblem receives the obtained decision variables and determines an extreme distribution of the probability density and adds it to the master problem. These two problems are computed alternately, and hence, the extreme distribution set in the master problem will cover enough extreme distributions to ensure the robustness of the dispatch. The computing framework of the two-stage solution is presented in Figure 2.

TABLE 1 Key parameters of the modern farm park.

Regulating resources	Parameters	Value
Day-ahead power trading	$[\underline{P}^{\mathrm{tr}}, \bar{P}^{\mathrm{tr}}]$/MW	[0, 2]
Intraday power trading	b_t^+, b_t^-(¥/MWh)	$1.5p_t$, $0.5p_t$
Biogas generator	$[\underline{P}^{\mathrm{g}}, \bar{P}^{\mathrm{g}}]$/MW	[0, 1.2]
	$bg\ t$/(¥/MWh)	80
	η^{p}, η^{h}	0.45, 0.351
Electric boiler	$\bar{H}^{\mathrm{b}}$/MW	0.8
	η^{b}	0.9
Transferable power load	d_t^+, d_t^-(¥/MWh)	10, 10
	$\Delta\bar{P}_t^{\mathrm{dr},+}, \Delta\bar{P}_t^{\mathrm{dr},-}$/MW	1, 1
	$T_{i,\mathrm{A}}$/h	13:00–17:00
Power storage	$\bar{P}^{\mathrm{s},+}, \bar{P}^{\mathrm{s},-}$/MW	0.3, 0.3
	$\underline{S}^{\mathrm{p}}, \bar{S}^{\mathrm{p}}$/MWh	[0, 0.6]
Heat storage	$\bar{H}^{\mathrm{s},+}, \bar{H}^{\mathrm{s},-}$/MW	[0.3, 0.3]
	$\underline{S}^{\mathrm{h}}, \bar{S}^{\mathrm{h}}$/MWh	[0, 0.6]

1) Master problem: the problem obtains the optimal solution against all known extreme distributions of the probability density.

$$\begin{aligned} f_{\mathrm{master}} = \min_{\boldsymbol{x}\in\chi} \quad & \boldsymbol{c}^{\top}\boldsymbol{x} + \pi \\ \text{s.t.} \quad & \pi \geq \sum_k p_{i,k} Q(\boldsymbol{x}, \boldsymbol{u}_k), \forall i \in \Lambda_{\nu-1} \end{aligned}, \tag{38}$$

where $\Lambda_{\nu-1}$ is the extreme distribution set revised from the previous step. Then, the optimal $\boldsymbol{x}$ is sent to the subproblem. The obtained objective is denoted as the lower bound (LB).

2) Subproblem: The problem determines an extreme distribution of the probability density with given $\boldsymbol{x}^{\star}$. The solution of the subproblem contains two steps. First, the optimal intraday cost of each reference sample is calculated:

$$\begin{aligned} Q(\boldsymbol{x}^{\star}, \boldsymbol{u}_k) = \min_{\boldsymbol{y}} \quad & \boldsymbol{f}^{\top}\boldsymbol{y} \\ \text{s.t.} \quad & \boldsymbol{G}\boldsymbol{y} \leq \boldsymbol{g} \\ & \boldsymbol{A}\boldsymbol{x}^{\star} + \boldsymbol{B}\boldsymbol{y} + \boldsymbol{C}\boldsymbol{u}_k = \boldsymbol{d} \end{aligned}. \tag{39}$$

Second, the expected intraday cost is maximized to determine an extreme distribution of the probability density:

$$f_{\mathrm{sub}} = \max_{p_k \in \mathcal{P}} \sum_k p_k Q(\boldsymbol{x}^{\star}, \boldsymbol{u}_k). \tag{40}$$

Then, the extreme distribution $\boldsymbol{p}$ of the probability density is added to the extreme distribution set, and the updated extreme distribution set is uploaded to the master problem. $\boldsymbol{c}^{\top}\boldsymbol{x}^{\star} + f_{\mathrm{sub}}$ is denoted as the upper bound (UB).

3) Convergence criterion check: end the iteration until the following convergence criterion; otherwise, go back to step 1 and modify $\nu = \nu+1$.

$$(\mathrm{UB} - \mathrm{LB}) \leq \varepsilon \mathrm{LB}, \tag{41}$$

where ε is a very small constant.

4 Numerical simulations

We take a modern farm park in Tsingtao city to validate the superiority of the constrained distributionally robust dispatch of the RIES. The day-ahead dispatch is performed for the next 0–24 h. All the programs are calculated with the CPLEX solver on a computer with an i7-1360P CPU. The power price in the day-ahead stage is displayed in Figure 3. The forecast information of photovoltaic energy, electric power, and heat load is presented in Figure 4, where the maximum prediction error is ±30% of the forecast value. The remaining parameters of the modern farm park are given in Table 1. Finally, the operational effectiveness of the dispatch plan is tested using the expected value of reference samples.

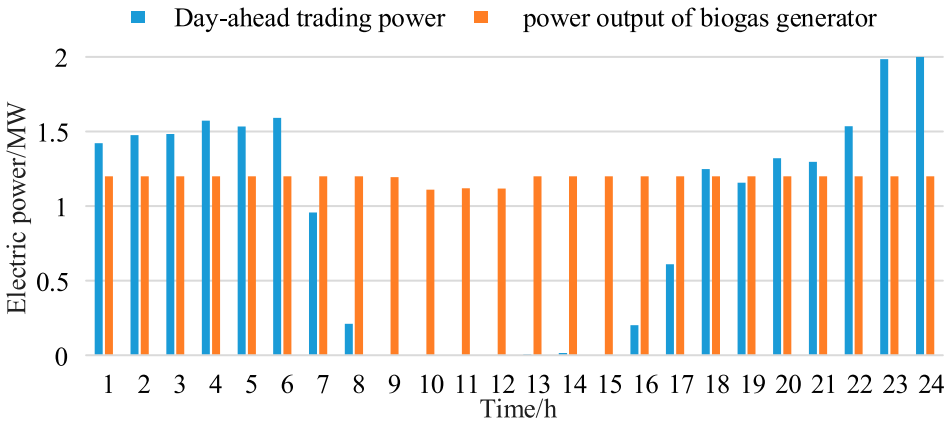

FIGURE 5
Day-ahead trading power and power output of the biogas generator.

10.3389/fenrg.2024.1411152

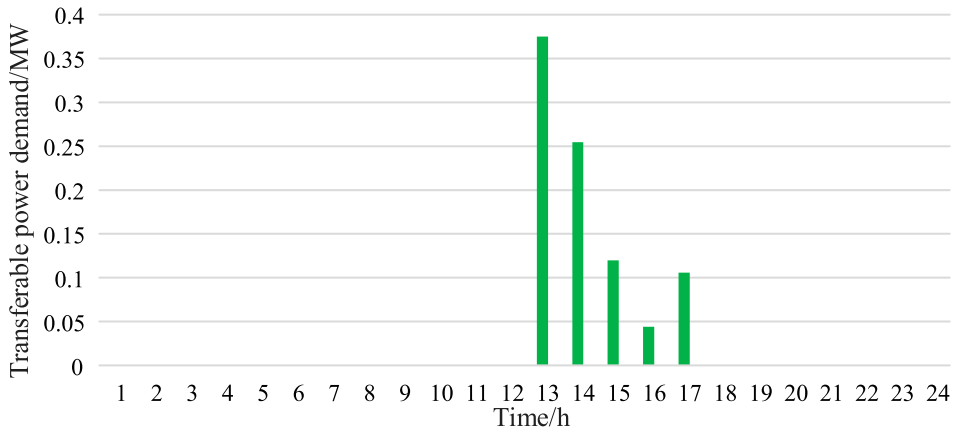

FIGURE 6
Distribution of transferable power load.

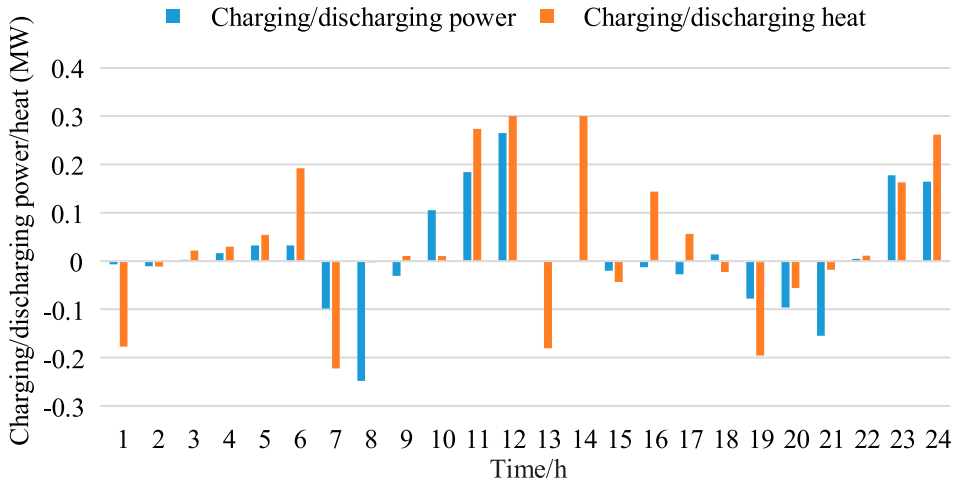

FIGURE 7
Charge–discharge state of power and heat storage.

TABLE 2 Comparison of the methods for uncertainty.

Methods	Optimized results		Monte Carlo simulation results	
	Cost/¥	Time/s	Empirical distribution cost/¥	Extreme distribution cost/¥
SO	12,935	2	12,935	13,497
RO	26,374	11	17,096	17,367
DRO	13,418	24	13,004	13,418
CDRO	13,461	20	12,943	13,461

4.1 Analysis for the dispatch plan

In the proposed dispatch model of the RIES, the decision variable $\boldsymbol{x}$ in the day-ahead stage is the trading power, while the intraday decision variables $\boldsymbol{y}$ is constituted by the dispatch plan of power storage, transferable power load, biogas generator, biogas storage, heat pump, electric boiler, and heat storage. Note that the following analysis for the intraday operation is presented with the expected value of the reference samples.

Figure 5 shows the day-ahead trading power and power export of the biogas generator. Due to the low power generation cost of the biogas unit, the power output of the biogas generator is always

TABLE 3 Comparison of the methods for uncertainty under different uncertainty degrees.

Uncertainty degree	Methods	Optimized results		Monte Carlo simulation results	
		Cost/¥	Time/s	Empirical distribution cost/¥	Extreme distribution cost/¥
0.75	SO	12,731	2	12,731	13,045
	DRO	13,014	28	12,761	13,014
	CDRO	13,030	14	12,734	13,030
1.00	SO	12,935	2	12,935	13,497
	DRO	13,418	24	13,004	13,418
	CDRO	13,461	20	12,943	13,461
1.25	SO	13,052	2	13,052	13,630
	DRO	13,559	23	13,104	13,559
	CDRO	13,592	16	13,057	13,592

TABLE 4 Optimization results related to the number of historical scenarios.

M	Obj./¥	Time/s
50	13,968	33
100	13,743	16
500	13,158	20
1,000	13,050	20
5,000	12,959	14
10,000	12,947	16

TABLE 5 Optimization results related to the number of reference samples.

K	Obj./¥	Time/s
10	12,811	8
30	13,046	10
50	13,461	20
100	14,020	40
150	14,139	42
200	14,350	45

TABLE 6 Optimization results related to the confidence degree.

α_∞	α_1		
	0.8	0.9	0.99
0.9	13347	13348	13348
0.95	13377	13384	13384
0.99	13436	13451	13463

maintained at a high level. At the dispatch periods t = 10:00–12:00, the power load is at the valley, while the available photovoltaic power output is at a relatively high level, which means that the net power load is at the lowest level during these periods, and hence, the power export of the biogas generator does not reach the maximum. Similarly, the RIES purchases very little electric power at the dispatch periods t = 8:00–16:00, with relatively lower net power load and heat load. During the dispatch periods t = 00:00–7:00 and 17:00–24:00, the power load and heat load are both at the peak while the photovoltaic power output is at the valley, and hence, the RIES purchases much electric power from the power market.

Figure 6 illustrates the distribution of transferable power load whose transferable periods are t = 13:00–17:00. The transferable power load is mostly transferred to t = 13:00–14:00 with lower power price, and thus, the operating cost of the RES is decreased.

Figure 7 shows the charge–discharge state of the power and heat storage, respectively. The power price is relatively low during the dispatch periods t = 1:00–6:00 and 23:00–24:00, and so, the power storage charges power. While the power price is relatively high during the dispatch periods t = 7:00–9:00 and 19:00–21:00, the power storage discharges power to supply the demand. Finally, during the dispatch periods t = 10:00–12:00, the power load is at the valley while the photovoltaic power output is at a relatively high level, and hence, the power storage charges power to accommodate photovoltaic power. As indicated from the above analysis, the energy storage flexibly charges and discharges power according to the power price, and hence can decrease the operating cost of the RIES. While for the heat storage, its charging and discharging status is similar to that of the power storage since the heat load is supported by the waste heat of the biogas generator and the electric boiler.

4.2 Comparison between different uncertainty methods

To verify the economy and robustness of the CDRO, this subsection compares the proposed method and the commonly used uncertainty methods, including SO, RO, and DRO. SO minimizes the operating cost expectation corresponding to the historical distribution of the source and load uncertainties, RO minimizes the operating cost corresponding to extreme scenarios,

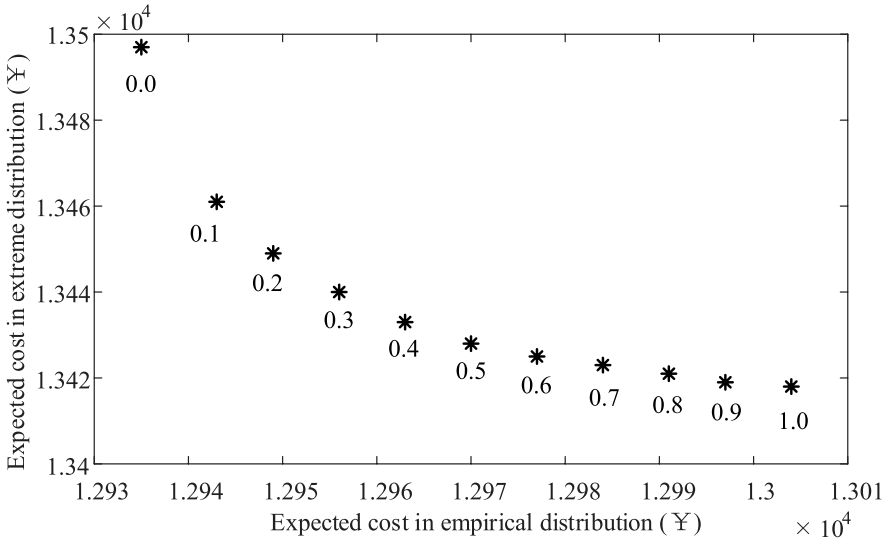

FIGURE 8
Optimization results related to the equilibrium coefficient.

TABLE 7 Computational efficiency of the two-stage solution.

Case		Iterations	Time/s
M	50	5	33
	1,000	4	20
	10,000	3	16
K	10	3	8
	100	4	40
	200	4	45

TABLE 8 Optimization results with different convergence gaps.

Convergence gap	Obj./¥	Iterations	Time/s
1e-3	13,460	3	17
1e-4	13,461	4	26
1e-5	13,461	4	26

and DRO minimizes the operating cost corresponding to extreme distributions. The proposed CDRO minimizes the operating cost expectation corresponding to extreme distributions while restricting the sacrifice of the operating cost expectation in the historical distribution. The comparison results related to these methods are shown in Table 2. As displayed in the table, SO has the lowest operating cost expectation in the historical distribution, while it is significantly less robust than DRO and CDRO under some extreme distributions. RO minimizes the operating cost corresponding to extreme scenarios, which is very conservative and relatively uneconomical since the probability of extreme scenarios is extremely low. Although the historical distribution cost of the CDRO is slightly higher than that of SO, its economical effectiveness under extreme distributions is significantly better than that of SO. Compared to SO, the historical distribution cost of CDRO is slightly sacrificed by 6.18E-04, while the cost efficiency under extreme distributions is significantly improved by 2.7E-03. In view of that the practical distribution of the source and load uncertainties does not strictly obey the empirical value, it is essential to address the distributional deviation and enhance the robustness of the dispatch plan.

To further verify the performance of the CDRO, we change the fluctuation degrees of source and load uncertainties, i.e., change to 0.75–1.25 times of the original. Since RO is very conservative, we compare the optimization results of SO, DRO, and CDRO. As shown in Table 3, no matter how the uncertainty degree changes, CDRO always achieves a tradeoff between the economical effectiveness and robustness, i.e., it sacrifices the historical distribution cost slightly to significantly improve the robustness. In addition, as the uncertainty degree increases, the advantage of CDRO in balancing the economical effectiveness and robustness becomes more obvious.

4.3 Sensitivity analysis related to the ambiguous set

The ambiguous set of the source and load uncertainties is related to the amount of historical scenarios (M), the amount of the reference sample (K), and the confidence degree (α_∞ and α_1). The default setting of M, K, θ_∞, and θ_1 in this paper is 200, 50, 0.99, and 0.95, respectively. This subsection will study the impact of these parameters on the optimization performance.

First, we study the influence of the amount of historical scenarios M on the optimization results. The optimization results with different M from 50 to 10,000 are displayed in Table 4. The results in the table reveal that the objective decreases with the

increase of the scale of historical observation. The reason is that the increase of historical observation limits the allowable gap of the probability distribution, and hence decreases the conservativeness of the proposed CDRO. It should be noted that the optimization results of CDRO actually approach that of SO with the increase of the scale of the historical observation, which further validates the flexibility of the proposed CDRO.

Second, we study the impact of the amount of reference samples K on the optimization results. The optimization results with different K from 10 to 200 are shown in Table 5. As K increases, the possible scenarios in the probability distribution of the source and load uncertainties are more dispersed, and hence, the maximum possible range of the probability distribution widens. Therefore, the optimized objective increases with the increase in the number of reference samples.

Finally, we study the impact of the confidence degree on the optimization performance, and the simulation results are displayed in Table 6. With the increase in the confidence degree α_∞ and α_1, the allowable gap of the probability density θ_∞ and θ_1 widens, and hence, the maximum possible range of the probability distribution widens. Therefore, the optimized objective increases with the increase in the confidence degree. It is worth noting that when $\alpha_\infty = 0.9$, the optimized objectives are the same for $\alpha_1 = 0.9$ and $\alpha_1 = 0.99$. As shown in Equations 30–33, only the infinity-norm works if the infinity-norm and 1-norm share the same confidence degree. At this time, even though the confidence degree for the 1-norm increases, the ambiguous set of the source and load uncertainties remains the same, and so, the optimized objective will not change.

4.4 Influence of the equilibrium coefficient

In the proposed CDRO, the equilibrium coefficient λ plays a crucial part in coordinating the economical effectiveness and the robustness of the dispatch plan. Figure 8 presents the operating cost expectation in the historical distribution and extreme distribution associated with the equilibrium coefficient within [0, 1]. As shown in the figure, if the equilibrium coefficient approaches 1, the operating cost expectation in the historical distribution increases, while the expected cost in extreme distribution decreases, which means that the CDRO pays more attention to the robustness than to economical effectiveness. When the equilibrium coefficient λ approaches 0, the operating cost expectation in the historical distribution increases and the expected cost in extreme distribution decreases, which means that the CDRO pays more attention to economical effectiveness than to robustness. In addition, when the equilibrium coefficient locates between 0 and 0.2, the expected cost in the extreme distribution significantly decreases with a very small loss of the operating cost expectation in the historical distribution, which means that the robustness can be ensured with a very slight sacrifice of economical effectiveness in common distributions. The above numerical results reveal that the CDRO can acquire a tradeoff between the robustness and economical effectiveness through a reasonable setting of the equilibrium coefficient. In practical applications, considering that historical distributions are more likely to occur while extreme distributions are less likely to occur, the proposed CDRO shall give priority to economical effectiveness in the historical distribution. Therefore, the equilibrium coefficient can be set within [0.1, 0.3] in practical applications.

4.5 Computational efficiency of the solution

The tailored two-stage solution procedure splits the dispatch problem to independently solvable master and subproblems. The master problem determines the day-ahead decision variables, and the subproblem determines an extreme distribution of the probability density. The iteration steps and computing time with different number of historical scenarios (M) and amount of reference samples (K) are displayed in Table 7. As indicated in the table, the iteration times of the proposed solution are few, and the calculation time is only tens of seconds, which validates the computational efficiency of the solution. In addition, the convergence of the two-stage solution is related to the convergence gap ε. We change the convergence gap and compare the optimization results. As shown in Table 8, the optimized objective descends when the convergence condition becomes strict. Although the iteration times and calculation time increase correspondingly, the computational efficiency of the proposed algorithm is still very high.

5 Conclusion

In this work, a constrained distributionally robust day-ahead dispatch model of a rural integrated energy system is developed, and a tailored two-stage solution is developed for the model. The rural system effectively coordinates the regulation resources such as trading power, biogas generator, electric boiler, transferable power load, power storage, and heat storage to reduce its operating cost. As indicated in the comparison with other uncertainty methods, the proposed constrained distributionally robust optimization (CDRO) sacrifices historical distributional cost slightly to improve its robustness. The ambiguous set of the source and load uncertainties influences the optimization performance of the proposed CDRO. When the scale of historical observation is large, the probability distribution range decreases, and the CDRO approaches SO. In addition, by reasonably setting the confidence level in the 1-norm and infinity-norm constraint, the conservativeness of CDRO can be reduced. The proposed CDRO fully combines the economical effectiveness of SO with the robustness of DRO and can achieve a tradeoff between economical effectiveness and robustness through a reasonable setting of the equilibrium coefficient.

Our future work will consider more regulating devices such as electricity-to-hydrogen devices and interruptible power load to improve the integrality of RIES modeling. In addition, the coordinated operation of the distribution network and multiple RIESs will be studied in the future.

Data availability statement

The original contributions presented in the study are included in the article/Supplementary Material; further inquiries can be directed to the corresponding author.

Author contributions

ZZ: methodology, writing–original draft, and writing–review and editing. SY: data curation and writing–review and editing. YM: formal analysis and writing–review and editing. SS: software, validation, and writing–review and editing. PY: data curation, investigation, and writing–review and editing. FY: formal analysis, validation, and writing–review and editing.

Funding

The author(s) declare that financial support was received for the research, authorship, and/or publication of this article. This work was sponsored by the Headquarters Science and Technology Project of State Grid Corporation of China, Research and application of distributed flexible low-carbon energy supply technology for rural distribution network (5108-202218280A-2-375-XG).

Conflict of interest

Authors ZZ, YM, and FY were employed by State Grid Shanghai Energy Internet Research Institute Co. Ltd. Authors SoY, SS, and PY were employed by State Grid Shandong Electric Power Company Electric Power Science Research Institute.

The authors declare that this study received funding from State Grid Corporation of China. The funder had the following involvement in the study: data collection and analysis.

Publisher's note

References

Bertsimas, D., Litvinov, E., Sun, X., Zhao, J., and Zheng, T. (2013). Adaptive robust optimization for the security constrained unit commitment problem. *IEEE Trans. Power Syst.* 28 (1), 52–63. doi:10.1109/TPWRS.2012.2205021

Bolurian, A., Akbari, H., and Mousavi, S. (2022). Day-ahead optimal scheduling of microgrid with considering demand side management under uncertainty. *Electr. Power Syst. Res.* 209, 107965. doi:10.1016/j.epsr.2022.107965

Ding, T., Yang, Q., Yang, Y., Li, C., Bie, Z., and Blaabjerg, F. (2017). A data-driven stochastic reactive power optimization considering uncertainties in active distribution networks and decomposition method. *IEEE Trans. Sustain. Energy* 9 (5), 4994–5004. doi:10.1109/TSG.2017.2677481

Eghbali, N., Hakimi, S. M., Hasankhani, A., Derakhshan, G., and Abdi, B. (2022). A scenario-based stochastic model for day-ahead energy management of a multi-carrier microgrid considering uncertainty of electric vehicles. *J. Energy Storage* 52, 104843. doi:10.1016/j.est.2022.104843

Fu, X., Zhou, Y., Sun, H., and Guo, Q. (2020). Online security analysis of a park-level agricultural energy Internet: review and prospect. *Proc. CSEE* 40 (17), 5404–5412. (in Chinese). doi:10.13334/j.0258-8013.pcsee.200108

Jani, A., Karimi, H., and Jadid, S. (2022). Two-layer stochastic day-ahead and real-time energy management of networked microgrids considering integration of renewable energy resources. *Appl. Energy* 323, 119630. doi:10.1016/j.apenergy.2022.119630

Liang, R., Yuan, L., Huang, H., Gu, C., Li, J., Lu, W., et al. (2024). Multi-hydraulic retention time rolling optimal operation method for rural biomass power generation system under uncertain temperature. *Proc. CSEE.* (in Chinese). doi:10.13334/j.0258-8013.pcsee.232154

Liu, Y., Guo, L., and Wang, C. (2018). Economic dispatch of microgrid based on two stage robust optimization. *Proc. CSEE* 38 (14), 4013–2022. (in Chinese). doi:10.13334/j.0258-8013.pcsee.170500

Ma, L., and Fu, X. (2021). Theory and application of agricultural energy Internet considering coupling of agriculture, meteorology and energy. *Electr. Power* 54 (11), 115–124. (in Chinese). doi:10.11930/j.issn.1004-9649.202006239

Qu, K., Zheng, X., Li, X., Lv, C., and Yu, T. (2022). Stochastic robust real-time power dispatch with wind uncertainty using difference-of-convexity optimization. *IEEE Trans. Power Syst.* 37 (6), 4497–4511. doi:10.1109/TPWRS.2022.3145907

Seyednouri, S. R., Safari, A., Farrokhifar, M., Ravadanegh, S. N., Quteishat, A., and Younis, M. (2023). Day-ahead scheduling of multi-energy microgrids based on a stochastic multi-objective optimization model. *Energies* 16 (4), 1802. doi:10.3390/en16041802

Siqin, Z., Niu, D., Wang, X., Zhen, H., Li, M., and Wang, J. (2022). A two-stage distributionally robust optimization model for P2G-CCHP microgrid considering uncertainty and carbon emission. *Energy* 260, 124796. doi:10.1016/j.energy.2022.124796

Tan, B., Chen, H., Zheng, X., and Huang, J. (2022). Two-stage robust optimization dispatch for multiple microgrids with electric vehicle loads based on a novel data-driven uncertainty set. *Int. J. Elec. Power* 134, 107359. doi:10.1016/j.ijepes.2021.107359

Wei, W., Liu, F., and Mei, S. (2016). Distributionally robust co-optimization of energy and reserve dispatch. *IEEE Trans. Sustain. Energy* 7 (1), 289–300. doi:10.1109/TSTE.2015.2494010

Wu, T., Bu, S., Wei, X., and Zhou, B. (2021). Multitasking multi-objective operation optimization of integrated energy system considering biogas-solar-wind renewables. *Energy Convers. Manag.* 229, 113736. doi:10.1016/j.enconman.2020.113736

Xu, J., Yi, X., Sun, Y., Lan, T., and Sun, H. (2017). Stochastic optimal scheduling based on scenario analysis for wind farms. *IEEE Trans. Sustain. Energy* 8 (4), 1548–1559. doi:10.1109/TSTE.2017.2694882

Yu, Y., and Yin, S. (2023). Incentive mechanism for the development of rural new energy industry: new energy enterprise–village collective linkages considering the quantum entanglement and benefit relationship. *Int. J. Energy Res.* 2023, 1–19. doi:10.1155/2023/1675858

Yu, Y., Yin, S., and Zhang, A. (2022). Clean energy-based rural low carbon transformation considering the supply and demand of new energy under government participation: a three-participators game model. *Energy Rep.* 8, 12011–12025. doi:10.1016/j.egyr.2022.09.037

Zhai, J., Wang, S., Guo, L., Jiang, Y., Kang, Z., and Jones, C. (2022). Data-driven distributionally robust joint chance-constrained energy management for multi-energy microgrid. *Appl. Energy* 326, 119939. doi:10.1016/j.apenergy.2022.119939

Zhang, K., Troitzsch, S., and Han, X. (2022). Distributionally robust co-optimized offering for transactive multi-energy microgrids. *Int. J. Elec. Power* 143, 108451. doi:10.1016/j.ijepes.2022.108451

Zhao, Z., Liu, Y., Guo, L., Bai, L., and Wang, C. (2021). Locational marginal pricing mechanism for uncertainty management based on improved multi-ellipsoidal uncertainty set. *J. Mod. Power Syst. Clean. Energy* 9 (4), 734–750. doi:10.35833/MPCE.2020.000824

Zheng, X., Qu, K., Lv, J., Li, Z., and Zeng, B. (2021). Addressing the conditional and correlated wind power forecast errors in unit commitment by distributionally robust optimization. *IEEE Trans. Sustain. Energy* 12 (2), 944–954. doi:10.1109/TSTE.2020.3026370

Zhou, B., Xu, D., Li, C., Chuang, C. Y., Cao, Y., Chan, K. W., et al. (2018). Optimal scheduling of biogas-solar-wind renewable portfolio for multicarrier energy supplies. *IEEE Trans. Power Syst.* 33 (6), 6229–6239. doi:10.1109/TPWRS.2018.2833496

Zuo, J., Xu, C., Wang, W., and Ji, Y. (2023). Distributionally robust optimization for virtual power plant clusters considering carbon emission-based dynamic dispatch priority. *Front. Energy Res.* 11. doi:10.3389/fenrg.2023.1214263

Nomenclature

Indexes and sets

t	Index of dispatch periods
k	Index of the reference sample
v	Step index in two-stage optimization
$\mathcal{P}$	Ambiguous set of source–demand uncertainty
Λ_v	Worst-case distribution set
$T_{i,\mathrm{A}}$	Set of transferable periods
$T_{i,\mathrm{B}}$	Set of non-transferable periods

Parameters

p_t	Day-ahead power price
$\underline{P}^{\mathrm{tr}}/\bar{P}^{\mathrm{tr}}$	Lower/upper restriction of day-ahead trading power
b_t^+/b_t^-	Intraday purchase/sale power price
b_t^{g}	Material cost coefficient of the biogas generator
d_t^+/d_t^-	Upward/downward cost coefficient of transferable power load
$\tilde{P}_t^{\mathrm{v}}$	Forecast value of photovoltaic power
$\tilde{P}_t^{\mathrm{d}}$	Forecast value of power load
$\tilde{H}_t^{\mathrm{d}}$	Forecast value of heat load
H	Calorific value of biogas
η^{p}, η^{h}	Generation efficiency and afterheat efficiency of the biogas generator
$\bar{P}^{\mathrm{g}}/\underline{P}^{\mathrm{g}}$	Upper/lower bound of power output of the biogas generator
η^{b}	Conversion efficiency of the electric boiler
$\Delta\bar{P}_t^{\mathrm{dr},+}$	Limit for upward regulation of transferable power load
$\Delta\bar{P}_t^{\mathrm{dr},-}$	Limit for downward regulation of transferable power load
$P_t^{\mathrm{dr},0}$	Base value of transferable power demand
$\bar{P}^{\mathrm{s},+}$, $\bar{P}^{\mathrm{s},-}$	Upper restriction for charging and discharging power of power storage
$\underline{S}^{\mathrm{p}}/\bar{S}^{\mathrm{p}}$	Lower/upper restrictions for stored power of power storage
$\eta^{\mathrm{p},+}/\eta^{\mathrm{p},-}$	Charging/discharging efficiency of power storage
S_0^{p}	Initial state of power storage
$\bar{H}^{\mathrm{s},+}$, $\bar{H}^{\mathrm{s},-}$	Upper limit for charging/discharging heat of heat storage
$\underline{S}^{\mathrm{h}}/\bar{S}^{\mathrm{h}}$	Lower/upper restrictions for stored heat of heat storage
$\eta^{\mathrm{h},+}/\eta^{\mathrm{h},-}$	Charging/discharging efficiency of heat storage
ρ	Heat loss rate of heat storage
S_0^{h}	Initial state of heat storage
$\bar{F}$	Allowed maximum for the expected cost in the historical distribution
λ	Equilibrium coefficient
u_k	The kth reference sample
$\underline{F}_{\mathrm{emp}}$	Empirical cost expectation obtained by SO
$\bar{F}_{\mathrm{emp}}$	Empirical cost expectation obtained by DRO
θ_{∞}, θ_1	Maximum gap in infinity-norm and 1- norm
α_{∞}, α_1	Confidence level in infinity-norm and 1- norm
M	Amount of historical scenarios
K	Amount of reference samples
$p_{k,0}$	Baseline probability density of the reference sample
ε	Convergence gap

Decision variables

P_t^{tr}	Day-ahead trading power
$\Delta P_t^{\mathrm{tr},+}$	Intraday purchase power
$\Delta P_t^{\mathrm{tr},-}$	Intraday sale power
$\Delta P_t^{\mathrm{dr},+}$	Upward regulation of transferable power load
$\Delta P_t^{\mathrm{dr},-}$	Downward regulation of transferable power load
G_t	Biogas input of the biogas generator
P_t^{g}, H_t^{g}	Power and afterheat produced by the biogas generator
H_t^{w}	Heat output of waste heat recovery
H_t^{b}, P_t^{b}	Heat output and power input of the electric boiler
$P_t^{\mathrm{s},+}/P_t^{\mathrm{s},-}$	Charging/discharging power of power storage
S_t^{p}	Stored power in power storage
$H_t^{\mathrm{s},+}/H_t^{\mathrm{s},-}$	Charging/discharging heat of heat storage
S_t^{h}	Stored heat in heat storage
x	Day-ahead decision variables
y	Intraday decision variables

Uncertain variables

u_t^{v}	Fluctuation of photovoltaic power
u_t^{p}	Fluctuation of power load
u_t^{h}	Fluctuation of heat load
p_k	Actual probability density of the kth reference sample

Acronyms

RIES	Rural integrated energy system
CDRO	Constrained distributionally robust optimization
SO	Stochastic optimization
RO	Robust optimization
DRO	Distributionally robust optimization
C&CG	Column and constraint generation